Hindawi
Advances in High Energy Physics
Volume 2017, Article ID 3802381, 10 pages
https://doi.org/10.1155/2017/3802381

*Research Article*

# Predictions for the Isolated Prompt Photon Production at the LHC at $\sqrt{s} = 13$ TeV

**Muhammad Goharipour and Hossein Mehraban**

*Faculty of Physics, Semnan University, P.O. Box 35131-19111, Semnan, Iran*

Correspondence should be addressed to Muhammad Goharipour; muhammad.goharipour@gmail.com

Received 22 September 2016; Revised 2 February 2017; Accepted 28 February 2017; Published 12 March 2017

Academic Editor: Anna Cimmino



The prompt photon production in hadronic collisions has a long history of providing information on the substructure of hadrons and testing the perturbative techniques of QCD. Some valuable information about the parton densities in the nucleon and nuclei, especially of the gluon, can also be achieved by analysing the measurements of the prompt photon production cross section whether inclusively or in association with heavy quarks or jets. In this work, we present predictions for the inclusive isolated prompt photon production in pp collisions at center-of-mass energy of 13 TeV using various modern PDF sets. The calculations are presented as a function of both photon transverse energy $E_T^\gamma$ and pseudorapidity $\eta^\gamma$ for the ATLAS kinematic coverage. We also study in detail the theoretical uncertainty in the cross sections due to the variation of the renormalization, factorization, and fragmentation scales. Moreover, we introduce and calculate the ratios of photon momenta for different rapidity regions and study the impact of various input PDFs on such quantity.

## 1. Introduction

From past to present, prompt photon production at hadron colliders has undergone very impressive experimental [1–18] and theoretical [19–41] developments. The experimental measurements cover a large domain of center-of-mass energy and also a wide range of photon transverse energy $E_T^\gamma$. The prompt photon production cross section at the LHC [11–16] has a significantly higher magnitude when compared to the Tevatron [3–10]. It is also much larger than the photoproduction cross section at HERA [42–44]. By definition, "prompt photons" are those photons that come from the collision of two primary partons in the protons, that is, photons not originating from hadron decays. The study of such photons provides a probe of perturbative Quantum Chromodynamics (pQCD) and measurement of their production cross sections, because of the sensitivity of the process to the gluon content of the nucleon, can provide useful information about the gluon parton distribution function (PDF) [45–49]. The associated production of prompt photons and heavy quarks, where the heavy quarks are either charm or bottom, can also provide a powerful tool for searching the intrinsic heavy quark components of the nucleon [50–52]. Moreover, a better understanding of prompt photon production is essential to have accurate QCD predictions for physical processes for which the prompt photons represent an important background such as diphoton decays of the Higgs boson [53–56].

Inclusive prompt photon production consists of two types of photons: direct and fragmentation photons [30]. Direct photons are those produced predominantly from initial hard scattering processes of the colliding quarks or gluons. Fragmentation photons are produced as bremsstrahlung emitted by a scattered parton, from the fragmentation of quarks and gluons. In this way, the fragmentation contribution of the inclusive prompt photon production is expressed as a convolution of the hard parton spectra with the nonperturbative fragmentation functions (FFs). An isolation requirement is used to reject the contamination from the dominant background of photons originating from hadron decays. As will be discussed later, imposing an isolation cut for the photons also reduces the fragmentation contribution so that the prompt photon cross section will be more sensitive to the direct component.

The production of photons in heavy-ion collisions [57–67] looks a promising future tool for studying the cold nuclear matter effects [68, 69], since photons are not accompanied by any final state interaction and hence leave the system with their energy and momenta unaltered. It has also been recognised as a powerful tool to study the fundamental properties of quark-gluon plasma (QGP) created in these collisions [70–76]. Furthermore, since the nuclear parton distribution functions (nPDFs) [77–82] (especially of the gluon) cannot be well determined using the available nuclear deep inelastic scattering (DIS) and Drell-Yan experimental data compared with the PDFs of the free nucleon, the measurements of prompt photon production in heavy-ion collisions can be used to constrain the gluon distributions within nuclei [83–86]. One of the important questions in the theoretical calculation of the particle production cross sections in nuclear collisions is that whether the factorization theorem [87–90] of collinear singularities is valid or not in this case (note that it is established in the case of hadronic collisions). So, the production of photons in nuclear collisions can also be recognised as a useful tool to answer this question.

Although in [48] the authors found a small effect on the gluon density due to the inclusion of large number of isolated prompt photon production data until 2012 related to the various experiments at different center-of-mass energies in a global analysis of PDFs, it is expected that the recent ATLAS data [16] measured at center-of-mass energy $\sqrt{s} = 8$ TeV can be used to improve PDF fits especially at larger Bjorken scaling variable $x$ where the PDF uncertainties are relatively large [35]. Such expectation can be accounted for near future ATLAS measurements at 13 TeV [91]. In this work, we are going to make predictions for the isolated prompt photon production in pp collisions at $\sqrt{s} = 13$ TeV using various modern PDF sets [92–94].

The paper is organised as follows. In Section 2, we first describe briefly the prompt photon physics and introduce various prescription of photon isolation. Then, using various modern PDF sets, we present the theoretical predictions for the isolated prompt photon production at 13 TeV to study the impact of input PDFs on the obtained results. The differential cross sections are presented as a function of both $E_T^\gamma$ and photon pseudorapidity $\eta^\gamma$. In Section 3, we study in detail the theoretical uncertainty in the cross sections due to the variation of the renormalization, factorization, and fragmentation scales and determine its order of magnitude. In Section 4, we introduce and calculate the ratios of photon momenta for different rapidity regions and study the impact of various input PDFs on such quantity. Finally, our results and conclusions are summarized in Section 5.

## 2. Predictions for the Isolated Prompt Photon Production at 13 TeV

Theoretical and computational aspects of the inclusive isolated prompt photon production such as involved leading order (LO) and next-to-leading order (NLO) subprocesses, direct and fragmentation component of the cross section, and photon isolation requirement have been discussed in many papers (e.g., see [30, 32]). Generally, the prompt photon cross section can be calculated by convolving nonperturbative PDFs and FFs with a perturbative partonic cross section by virtue of the factorization theorem. Actually, as mentioned in the Introduction, there are two components contributing to the prompt photon cross section: direct and fragmentation parts. In view of the theoretical calculations, they can be computed separately, though they cannot be measured separately in the experiments. Accordingly, the prompt photon cross section in hadronic collisions can be written as follows:

$$d\sigma^{\gamma+X} = d\sigma^{\gamma+X}_{\text{dir}} + d\sigma^{\gamma+X}_{\text{fragm}}, \tag{1}$$

where the first and second terms represent the direct and fragmentation contributions, respectively, and $X$ indicates the inclusive nature of the cross section as usual.

There are three scales that should be set in the calculation of the cross section equation (1). For the direct part, the renormalization scale $\mu$ appears in perturbative partonic cross section while the (initial state) factorization scale $M$ appears in both partonic cross section and PDFs. For the fragmentation part, in addition to $\mu$ and $M$, the partonic cross section includes also the fragmentation scale $M_F$ (final state factorization scale for the fragmentation process). In this case, $M_F$ also appears in the parton-to-photon fragmentation functions. Note that, whether for direct or fragmentation components, the renormalization scale $\mu$ appears in the strong coupling constant $\alpha_s$. In theoretical calculations of the prompt photon production, some uncertainties come from scale variations. We study in detail these uncertainties for the isolated prompt photon production at 13 TeV in the next section.

At LO, there are two Born-level subprocesses contributing to the prompt photon production cross section: the quark-gluon Compton scattering $q(\overline{q})g \to \gamma q(\overline{q})$ or quark-anti-quark annihilation $q\overline{q} \to \gamma g$. Although at NLO there are more contributing subprocesses $q(\overline{q})g \to \gamma g q(\overline{q})$ and $q\overline{q} \to \gamma g g$ and the others from the virtual corrections to the Born-level processes, the point-like coupling of the photon to quarks makes the calculations easier [19, 20, 29] (note that the first calculation of direct photon production at next-to-next-to-leading order (NNLO) accuracy in QCD has also been presented recently [40]). It is established that the $q\overline{q}$ annihilation channel is suppressed compared to the other subprocesses at pp colliders such as LHC and RHIC whereas, at the Tevatron that is a $p\overline{p}$ collider, this channel is relevant [47].

For measuring the prompt photon production at hadron colliders inclusively, the background of secondary photons coming from the decays of hadrons produced in the collision should be well rejected. We can do it by imposing appropriate isolation cuts. As mentioned, the photon isolation also significantly reduces the fragmentation components of the prompt photon cross section. Actually, the reason is that the fragmentation photons are emitted collinearly to the parent parton, and on the other hand, the isolation cut discards the prompt photon events that have too much hadronic activity. Here we introduce two prescriptions of photon isolation used so far in photon production studies. The most used is the cone criterion [30] that is defined as follows. A photon is isolated

if, inside a cone of radius $R$ centered around the photon direction in the rapidity $y$ and azimuthal angle $\phi$ plane, the amount of hadronic transverse energy $E_T^{\text{had}}$ is smaller than some value $E_T^{\text{max}}$:

$$E_T^{\text{had}} \leq E_T^{\text{max}}, \qquad \left(y - y_\gamma\right)^2 + \left(\phi - \phi_\gamma\right)^2 \leq R^2. \tag{2}$$

Although both the CMS and ATLAS collaborations take $R = 0.4$, the value of $E_T^{\text{max}}$ is different in their various measurements. For example, it is a finite value 5 GeV in the CMS measurement [12] or 7 GeV in the ATLAS measurement [15] both at $\sqrt{s} = 7$ TeV whereas it has been considered as a function of photon transverse energy $E_T^\gamma$ as $E_T^{\text{max}} = 4.8\,\text{GeV} + 0.0042E_T^\gamma$ in the recent ATLAS measurement at $\sqrt{s} = 8$ TeV [16]. In another prescription of photon isolation proposed by Frixione [97], the fragmentation components are suppressed while the cross section is kept infrared safe at any order in perturbative QCD. In this case, the amount of $E_T^{\text{had}}$ is required to satisfy the condition $E_T^{\text{had}} \leq f(r)$, for all radii $r$ inside the cone described in (2). The energy profile function $f(r)$ can be considered as

$$f(r) = \epsilon_s E_{\text{T}}^\gamma \left(\frac{1 - \cos(r)}{1 - \cos(R)}\right)^n, \tag{3}$$

where $\epsilon_s$ and $n$ are positive numbers of order one. Note that $f(r)$ is an increasing function of $r$ and falls to zero as $r \to 0$, since $n$ is positive.

There are some computer codes that can be used to calculate the prompt photon production cross section at NLO such as JetPhox [30, 32, 98] and PeTeR [99]. JetPhox is a Monte Carlo programme written as a partonic event generator for the prediction of processes with photons in the final state. It can calculate the direct and fragmentation contributions of the cross section, separately. The calculation can be configured to specify several parameters like kinematic range, PDFs, and FFs and also to use an isolation cut with a finite value or $E_T^\gamma$ dependent linear function for $E_T^{\text{max}}$ in (2).

Now we are in position to predict the isolated prompt photon production in pp collisions at center-of-mass energy of 13 TeV using various modern PDF sets (CT14 [92], MMHT14 [93], NNPDF3.0 [94], HERAPDF2.0 [95], and JR14 [96]). In this way, we can also investigate the effect of the PDF choice on the predictions. Note that, for each group, its NLO PDF sets with $\alpha_s(M_Z) = 0.118$ are taken through the LHAPDF package [100]. It should be also noted that we use the kinematic settings introduced in [91]. All calculations in this work are performed using the JetPhox with including all diagrams up to the LO and NLO order of QED and QCD coupling, respectively, defined in the $\overline{\text{MS}}$ renormalization scheme (it is worth pointing out in this context that since the NNLO calculations [40] have not yet been incorporated into any readily available codes like JetPhox, the NLO results are still interesting). The fine-structure constant ($\alpha_{\text{EM}}$) is set to the JetPhox default of 1/137. Moreover, for calculating the fragmentation component of the cross sections, we use in all predictions the NLO Bourhis-Fontannaz-Guillet FFs of photons [101]. The isolation transverse energy is taken to be $E_T^\gamma$ dependent as $E_T^{\text{max}} = 4.8\,\text{GeV} + 0.0042E_T^\gamma$ [91]. In all calculations that are performed in this section, the renormalization ($\mu$), factorization ($M$), and fragmentation ($M_F$) scales are set to the photon transverse energy ($\mu = M = M_F = E_T^\gamma$) and the scale uncertainty is studied separately in the next section.

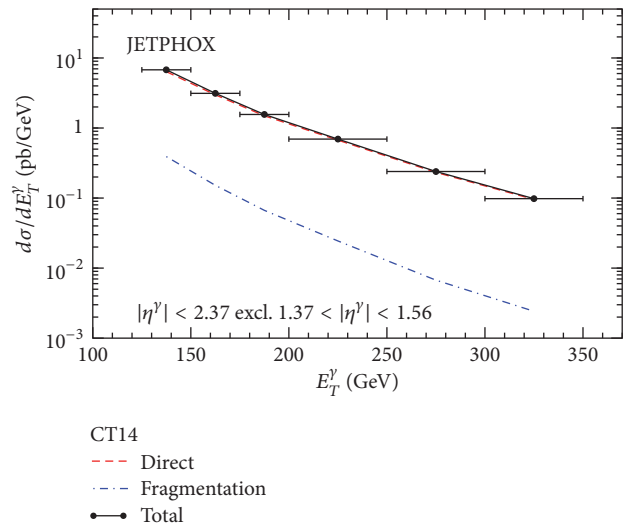


Figure 1: The NLO differential cross section of the isolated prompt photon production in pp collisions at $\sqrt{s} = 13$ TeV as a function of $E_T^\gamma$ in the kinematic range $125 < E_T^\gamma < 350$ GeV for $|\eta^\gamma| < 2.37$ excluding the region $1.37 < |\eta^\gamma| < 1.56$ and using NLO CT14 [92] PDFs. The direct (red dashed curve) and fragmentation (blue dotted-dashed curve) contributions to the total cross section (black solid curve) have been shown, separately.

As a first step, we calculate the NLO differential cross section of the isolated prompt photon production in pp collisions at $\sqrt{s} = 13$ TeV as a function of $E_T^\gamma$ in the kinematic range $125 < E_T^\gamma < 350$ GeV for $|\eta^\gamma| < 2.37$ excluding the region $1.37 < |\eta^\gamma| < 1.56$. It should be noted here that photons are detected in ATLAS by a lead-liquid Argon sampling electromagnetic calorimeter (ECAL) with an accordion geometry, divided into three sections: a barrel section covering the pseudorapidity region $|\eta^\gamma| < 1.475$ and two endcap sections covering the pseudorapidity regions $1.375 < |\eta^\gamma| < 3.2$. Measurement of the isolated prompt photon production with the ATLAS detector is usually performed for $|\eta^\gamma| < 2.37$ excluding the region $1.37 < |\eta^\gamma| < 1.56$ to include the detector region equipped with tracking detectors, but ignoring the transition region between the barrel and endcap calorimeters where the detector response is not optimal [14–16]. Figure 1 shows the obtained results using CT14 PDFs [92] for direct (red dashed curve) and fragmentation (blue dotted-dashed curve) contributions to the cross section and also total cross section (black solid curve), separately. Note that the horizontal error bars show the edges of each bin in $E_T^\gamma$ and the theoretical uncertainties in the results are discussed separately in the next section. This figure indicates that the direct component dominates completely the cross section, in all ranges of $E_T^\gamma$ especially at larger values. To be more

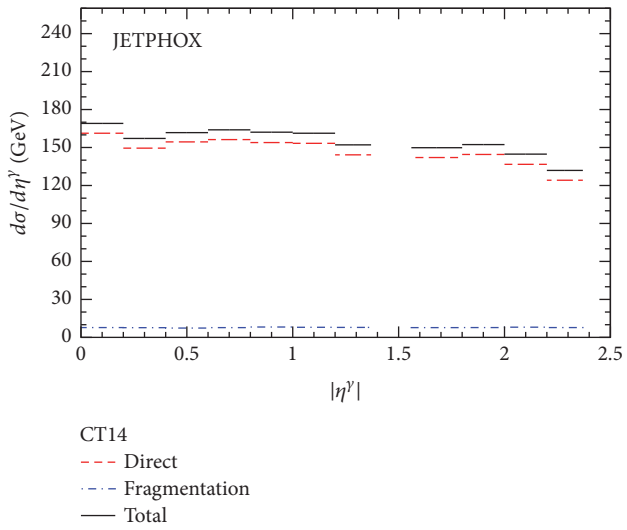


FIGURE 2: Same as Figure 1, but as a function of $\eta^\gamma$.

precise, the contribution of the fragmentation component to the total cross section is of the order of 5% at smallest value of $E_T^\gamma$ and even less than 3% at larger ones. This fact can be very important in view of the phenomenology, because we can use the future ATLAS data at $\sqrt{s} = 13$ in a new global analysis of PDFs without considering the fragmentation component, since its calculation can be time consuming and also adds FFs uncertainties in the analysis (note that our present knowledge of photon fragmentation functions is not satisfactory enough).

By virtue of the JETPHOX facilities, we can also calculate the NLO differential cross section of the isolated prompt photon production in pp collisions at $\sqrt{s} = 13$ TeV as a function of photon pseudorapidity $\eta^\gamma$. The obtained results using CT14 PDFs for $125 < E_T^\gamma < 350$ GeV and both $|\eta^\gamma| < 1.37$ and $1.56 < |\eta^\gamma| < 2.37$ regions have been shown in Figure 2 where we have again plotted both the direct (red dashed curve) and fragmentation (blue dotted-dashed curve) parts and also total cross section (black solid curve), for comparison. In this case, the contribution of the fragmentation component to the cross section is either about 5% at all values of $\eta^\gamma$ or then completely negligible compared with the direct component.

In order to study the impact of input PDFs on the final results and estimate the order of magnitude of the difference between their predictions, we can now recalculate the differential cross sections presented in Figures 1 and 2, but this time using other PDF sets. To this aim, we choose the NLO MMHT14 [93], NNPDF3.0 [94], HERAPDF2.0 [95], and JR14 [96] PDF sets (it should be noted that we use the dynamical PDFs set of JR14). Figures 3 and 4 show the comparison between their predictions for the total differential cross section of the isolated prompt photon production in pp collisions at $\sqrt{s} = 13$ TeV as a function of $E_T^\gamma$ and $\eta^\gamma$ for the same kinematic settings as Figures 1 and 2, respectively. The difference between the predictions in the various kinematic regions can be investigated in more detail from the bottom panel of each figure where the ratios of all

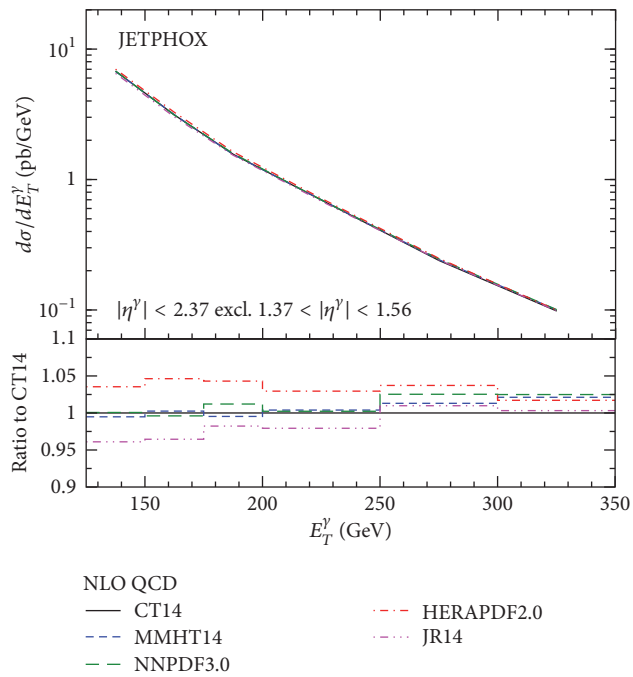


FIGURE 3: A comparison of the NLO theoretical predictions for the total differential cross section of the isolated prompt photon production as a function of $E_T^\gamma$ using various NLO PDFs of CT14 [92] (black solid curve), MMHT14 [93] (blue dashed curve), NNPDF3.0 [94] (green long-dashed curve), HERAPDF2.0 [95] (red dotted-dashed curve), and JR14 [96] (pink dotted-dotted-dashed curve) at $\sqrt{s} = 13$ TeV in the kinematic range $125 < E_T^\gamma < 350$ GeV for $|\eta^\gamma| < 2.37$ excluding the region $1.37 < |\eta^\gamma| < 1.56$. Ratio to the central value of CT14 has been shown in the bottom panel.

predictions to the central value of CT14 have been shown. As can be seen, for both cross sections, all predictions are in good agreement with each other so that, for example, the CT14, MMHT14, and NNPDF3.0 are the same to a large extent at smaller values of $E_T^\gamma$ in Figure 3. However, the differences between the HERAPDF2.0 and JR14 predictions with CT14 are somewhat larger than the others at low $E_T^\gamma$. Overall, we can state that the difference between these PDF sets is up to 5%. This is due to the fact that the parton distributions from various PDF sets, especially of the gluon in this case, become very similar at very high energies. Note also that in view of the experimental uncertainties [91] the total systematic uncertainty is smaller than 5% at low values of $E_T^\gamma$ and it increases as $E_T^\gamma$ increases. Therefore, considering only the systematic uncertainty, discrimination between the theoretical predictions at the level of 5% is going to be possible just at low values of $E_T^\gamma$. However, although the systematic uncertainty dominates the total experimental uncertainty at low values of $E_T^\gamma$, the statistical uncertainty should also be considered as it increases towards high $E_T^\gamma$.

## 3. The Study of Scale Uncertainty

In the previous section we calculated the cross section of isolated prompt photon production in pp collisions using

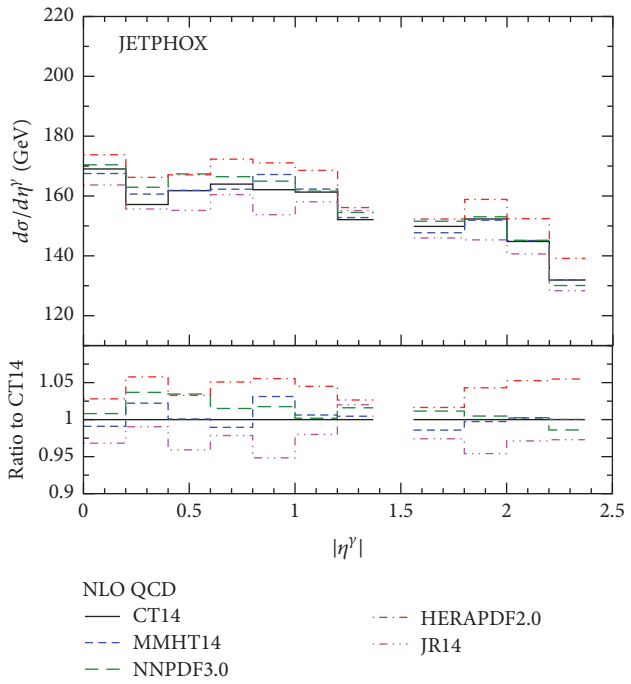


FIGURE 4: Same as Figure 3, but as a function of $\eta^\gamma$.

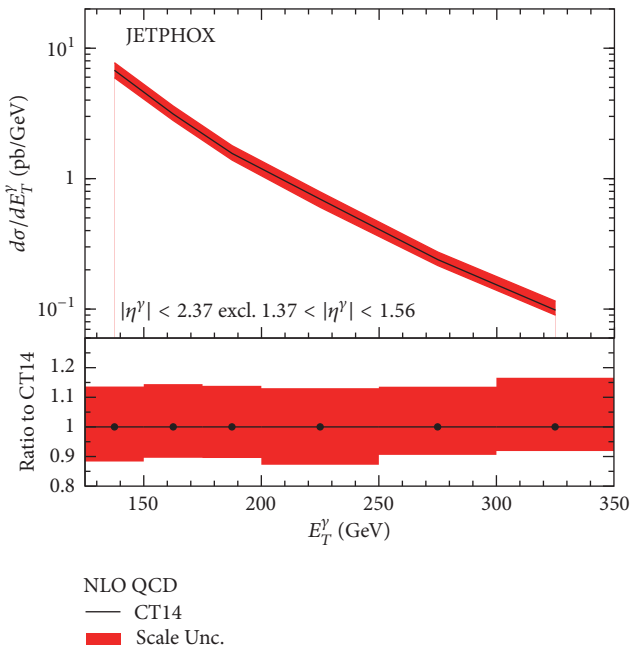


FIGURE 5: The NLO theoretical predictions for the total differential cross section of the isolated prompt photon as a function of $E_T^\gamma$ using NLO CT14 [92] PDFs with scale uncertainty (red band) at $\sqrt{s} = 13$ TeV in the kinematic range $125 < E_T^\gamma < 350$ GeV for $|\eta^\gamma| < 2.37$ excluding the region $1.37 < |\eta^\gamma| < 1.56$. Ratio to the central value of CT14 has been shown in the bottom panel.

various PDF sets. Now, it is important to calculate and study the theoretical uncertainties in the results. Since the dominant theoretical uncertainty is that arising from the scale uncertainties, in this section, we discuss only the scale uncertainties and ignore the study of PDFs uncertainties (note that the uncertainty arising from those in the PDFs amounts to 1–4%). As discussed in the previous section, the NLO calculation of the isolated prompt photon production involves all three renormalization ($\mu$), factorization ($M$), and fragmentation ($M_F$) scales. If we could calculate the cross section to all orders in perturbation theory, we could say that the cross section is scale independent and there is no theoretical uncertainty on the results due to the scales choice. But the scales choice becomes an important issue when we calculate the cross section to a fixed order in $\alpha_s$. Since the mentioned scales are all unphysical, the more reliable predictions are those for which the dependence of the cross section on the scales is minimised. It has been established that no optimal scale choice is possible for the prediction of the inclusive photon cross section in the region of the phase space of interest [102]. In this way, it was accepted that the predictions and their uncertainties should be made by setting all scales to be equal and varying them by a factor of 2 around the central value $\mu = M = M_F = E_T^\gamma$. However, if we want to be more correct in the calculation of the scale uncertainties, we should follow a method consisting of the combination of both incoherent and coherent scales variations [102]. To be more precise, in an incoherent variation one should vary the scales independently by a factor of 2 around the central value so that one scale is varied keeping the other two equal to $E_T^\gamma$. In a coherent variation one should vary the scales simultaneously by a factor of 2 around the central value as before. Then, the total scale uncertainty can be calculated by adding in quadrature all obtained uncertainties considering the following constraints:

(i) $\mu = M = M_F \in [E_T^\gamma/2, 2E_T^\gamma]$;

(ii) $\mu \in [E_T^\gamma/2, 2E_T^\gamma]$, $M = M_F = E_T^\gamma$;

(iii) $M \in [E_T^\gamma/2, 2E_T^\gamma]$, $\mu = M_F = E_T^\gamma$;

(iv) $M_F \in [E_T^\gamma/2, 2E_T^\gamma]$, $\mu = M = E_T^\gamma$.

In order to study the scale uncertainty of the isolated prompt photon production cross section in pp collisions at $\sqrt{s} = 13$ TeV, we again select the CT14 [92] PDFs and perform the calculations as a function of both $E_T^\gamma$ and $\eta^\gamma$ for the ATLAS kinematic [91]. Figures 5 and 6 show the obtained results where the predictions and scale uncertainties have been shown as black solid curves and red bands, respectively. The ratio to CT14 central prediction has been shown in the bottom panel of each figure. As one can see, the scale uncertainty can reach 20% in some regions. The large scale variations indicate that the NNLO calculations are needed to make more realistic theoretical predictions. Such calculations [40] are now becoming available and will be the subject of further work.

## 4. The Ratios of Photon Momenta for Different Rapidity Regions

As we saw in the previous section, if one considers the combination of both incoherent and coherent scale variations, the

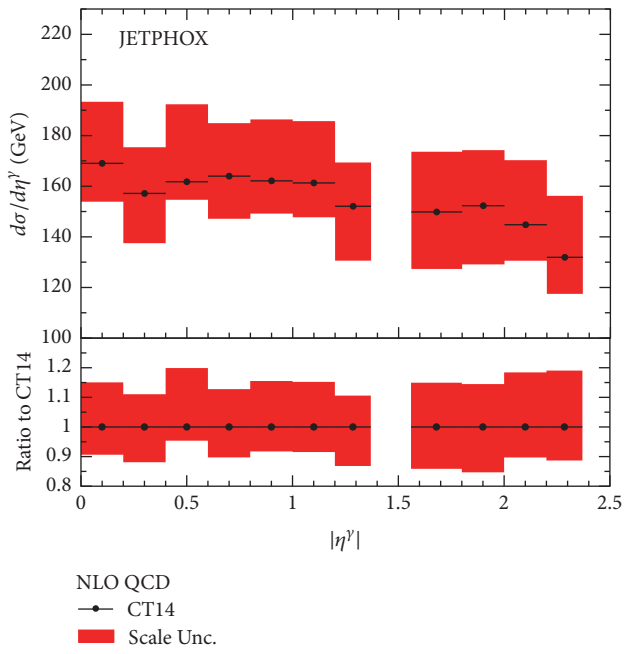


Figure 6: Same as Figure 5, but as a function of $\eta^\gamma$.

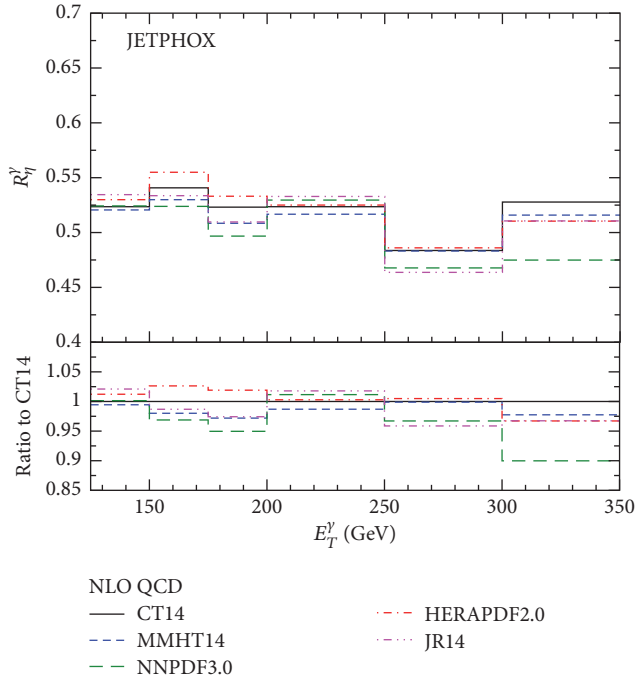


Figure 7: A comparison of the ratio of the NLO theoretical predictions for the differential cross section of the isolated prompt photon for the rapidity region $1.56 < |\eta^\gamma| < 2.37$ to the same ones but for the rapidity region $|\eta^\gamma| < 1.37$ as a function of $E_T^\gamma$ using various NLO PDFs of CT14 [92] (black solid curve), MMHT14 [93] (blue dashed curve), NNPDF3.0 [94] (green long-dashed curve), HERAPDF2.0 [95] (red dotted-dashed curve), and JR14 [96] (pink dotted-dotted-dashed curve) at $\sqrt{s} = 13$ TeV in the kinematic range $125 < E_T^\gamma < 350$ GeV for $|\eta^\gamma| < 2.37$ excluding the region $1.37 < |\eta^\gamma| < 1.56$. Ratio to the central value of CT14 has been shown in the bottom panel.

resulting scale uncertainty is considerably large. Generally, the decrease of the total uncertainty origination from various sources is a very important issue in both the experimental measurements and theoretical calculations. In most cases, the expression of results as ratios can be very useful to this aim. For example, in nuclear collisions, it is well established now that the measurement of nuclear modification and forward-to-backward ratios is more suitable than single differential cross section [85, 86]. In this section, we calculate and study the ratios of photon momenta for different rapidity regions using various input PDFs. Such ratios have the advantage of cancelling some theoretical and experimental uncertainties. Consider the relation

$$R_\eta^\gamma \equiv \frac{d\sigma/dE_T\big|_{\eta\in[\eta_1,\eta_2]}}{d\sigma/dE_T\big|_{\eta\in[\eta_3,\eta_4]}}, \tag{4}$$

in which $[\eta_1, \eta_2]$ and $[\eta_3, \eta_4]$ represent different rapidity regions. Note that since the differential cross section is sensitive to the different values of $x$ in different rapidity regions, then $R_\eta^\gamma$ can probe the input PDFs in a more curious way. Now, we calculate the ratios of the NLO theoretical predictions for the differential cross section of the isolated prompt photon for the rapidity region $1.56 < |\eta^\gamma| < 2.37$ to the same ones but for the rapidity region $|\eta^\gamma| < 1.37$. The calculations are performed again using NLO PDFs of CT14 [92], MMHT14 [93], NNPDF3.0 [94], HERAPDF2.0 [95], and JR14 [96] at $\sqrt{s} = 13$ TeV. Figure 7 shows the obtained results as a function of $E_T^\gamma$. The ratio to the central value of CT14 has been shown in the bottom panel. Compared with Figure 3 (see the bottom panel of two figures), the difference between the HERAPDF2.0 and JR14 predictions with the CT14 decreases at low values of $E_T^\gamma$ in this case. However, the NNPDF3.0 prediction is taken away from CT14 towards larger values of $E_T^\gamma$ so that the difference between them is reached even to 10%.

## 5. Summary and Conclusions

The study of the energetic photons produced in the collision of two hadrons provides a probe of perturbative QCD and can also give us some valuable information about the parton densities in the nucleon and nuclei especially of the gluon. Photon production in heavy-ion collisions is also a powerful tool to study the cold nuclear matter effects and the fundamental properties of QGP. It is indicated that the recent ATLAS data [16] measured at center-of-mass energy $\sqrt{s} = 8$ TeV can be used to improve PDF fits especially at larger Bjorken scaling variable $x$ [35]. So, the near future ATLAS measurement at 13 TeV [91] has more important role in this respect. In the present paper, we presented the theoretical predictions for the isolated prompt photon production in pp collisions at $\sqrt{s} = 13$ TeV as a function of both photon transverse energy $E_T^\gamma$ and pseudorapidity $\eta^\gamma$. All calculations were performed using the JetPhox with including all diagrams up to the LO and NLO order of QED and QCD coupling, respectively, defined in the $\overline{\text{MS}}$ renormalization scheme. The isolation

transverse energy is taken to be $E_T^\gamma$ dependent as $E_T^{\max} = 4.8\,\text{GeV} + 0.0042E_T^\gamma$ [91]. As a result, we found that the direct component dominates completely the cross section in both cases, so that the contribution of the fragmentation component to the total cross section is not more than 5% and is even reduced to 3% at some regions. So, we can study the impact of future ATLAS data at $\sqrt{s} = 13$ on PDFs in a new global analysis, neglecting the fragmentation component since its calculation can be time consuming and also adds FFs uncertainties in the analysis. Then we compared the predictions from various modern PDF sets, namely, the CT14 [92], MMHT14 [93], NNPDF3.0 [94], HERAPDF2.0 [95], and JR14 [96] to investigate the effect of the PDF choice on the cross sections. We found that all predictions are in good agreement with each other. To be more precise, overall, the greatest difference between them is about 5%. This can be attributed to the similarity of the parton distributions, especially of the gluon in this case, from various PDF sets at very high energies. In particular, the CT14, MMHT14, and NNPDF3.0 predictions are the same to a large extent at smaller values of $E_T^\gamma$ while the HERAPDF2.0 and JR14 predictions differ a little more with them. We also studied in detail the theoretical uncertainty in the cross sections due to the variation of the renormalization, factorization, and fragmentation scales. The method consists of the combination of both incoherent and coherent scales variations. We found that the scale uncertainty can reach 20% in some regions so the NNLO calculations are needed to make more realistic theoretical predictions. Finally, we calculated the ratios of photon momenta for different rapidity regions and studied the impact of various input PDFs on such quantity. It has the advantage of cancelling some theoretical and experimental uncertainties and can probe the input PDFs in a more curious way because the differential cross section is sensitive to the different values of $x$ in different rapidity regions.

## Conflicts of Interest

The authors declare that there are no conflicts of interest regarding the publication of this paper.

## References


[1] C. Albajar, M. G. Albrow, O. C. Allkofer et al., "Direct photon production at the CERN proton-antiproton collider," *Physics Letters B*, vol. 209, no. 2-3, pp. 385–396, 1988.

[2] J. Alitti, G. Ambrosini, R. Ansari et al., "A measurement of single and double prompt photon production at the CERN pp collider," *Physics Letters B*, vol. 288, no. 3-4, pp. 386–394, 1992.

[3] B. Abbott, M. Abolins, V. Abramov et al., "Isolated Photon Cross Section in $p\overline{p}$ Collisions at $\sqrt{s} = 1.8$ TeV," *Physical Review Letters*, vol. 84, no. 13, pp. 2786–2791, 2000.

[4] V. M. Abazov, B. Abbott, A. Abdesselam et al., "Ratio of Isolated Photon Cross Sections in $p\overline{p}$ Collisions at $\sqrt{s} = 360$ and 1800 GeV," *Physical Review Letters*, vol. 87, no. 28, Article ID 251805, 2001.

[5] V. M. Abazov, B. Abbott, M. Abolins et al., "Measurement of the isolated photon cross section in $p\overline{p}$ collisions at $\sqrt{s} = 1.96$ TeV," *Physics Letters B*, vol. 639, no. 3-4, pp. 151–158, 2006.

[6] V. M. Abazov, B. Abbott, M. Abolins et al., "Erratum to: Measurement of the isolated photon cross section in $p\overline{p}$ collisions at $\sqrt{s} = 1.96$ TeV," *Physics Letters B*, vol. 658, no. 5, pp. 285–289, 2008.

[7] D. Acosta, T. Affolder, H. Akimoto et al., "Comparison of the isolated direct photon cross sections in $p\overline{p}$ collisions at $\sqrt{s} = 1.8$ TeV and $\sqrt{s} = 0.63$ Tev," *Physical Review D*, vol. 65, no. 11, Article ID 112003, 10 pages, 2002.

[8] D. Acosta, T. Affolder, M. G. Albrow et al., "Direct photon cross section with conversions at CDF," *Physical Review D*, vol. 70, no. 7, Article ID 074008, 12 pages, 2004.

[9] T. Aaltonen, J. Adelman, B. Gonzalez et al., "Measurement of the inclusive isolated prompt photon cross section in $p\overline{p}$ collisions at $\sqrt{s} = 1.96$ TeV using the CDF detector," *Physical Review D*, vol. 80, Article ID 111106, 2009.

[10] A. Luca, "Measurement of the inclusive isolated prompt photon cross section in $p\overline{p}$ collisions at $\sqrt{s} = 1.96$ ~TeV, using the Full CDF Data Sample," FERMILAB-THESIS-2016-08, 2016.

[11] V. Khachatryan, A. M. Sirunyan, A. Tumasyan et al., "Measurement of the isolated prompt photon production cross section in $pp$ collisions at $\sqrt{s} = 7$ TeV," *Physical Review Letters*, vol. 106, Article ID 082001, 2011.

[12] S. Chatrchyan, A. Apresyan, A. Bornheim et al., "Measurement of the differential cross section for isolated prompt photon production in $pp$ collisions at 7 TeV," *Physical Review D*, vol. 84, no. 5, Article ID 052011, 2011.

[13] G. Aad, B. Abbott, J. Abdallah et al., "Measurement of the inclusive isolated prompt photon cross section in $pp$ collisions at $\sqrt{s} = 7$ TeV with the ATLAS detector," *Physical Review D*, vol. 83, no. 5, Article ID 052005, 31 pages, 2011.

[14] G. Aad, B. Abbott, J. Abdallah et al., "Measurement of the inclusive isolated prompt photon cross-section in $pp$ collisions at $\sqrt{s} = 7$ TeV using 35 pb−1 of ATLAS data," *Physics Letters B*, vol. 706, no. 2-3, pp. 150–167, 2011.

[15] G. Aad, T. Abajyan, B. Abbott et al., "Measurement of the inclusive isolated prompt photons cross section in $pp$ collisions at $\sqrt{s} = 7$ TeV with the ATLAS detector using 4.6 fb$^{-1}$," *Physical Review D*, vol. 89, no. 5, Article ID 052004, 24 pages, 2014.

[16] G. Aad, B. Abbott, J. Abdallah et al., "Measurement of the inclusive isolated prompt photon cross section in $pp$ collisions at $\sqrt{s} = 8$ TeV with the ATLAS detector," *JHEP*, vol. 1608, article 005, 2016.

[17] S. S. Adler, S. Afanasiev, C. Aidala et al., "Measurement of direct photon production in $p+p$ collisions at $\sqrt{s} = 200$ GeV," *Physical Review Letters*, vol. 98, no. 1, Article ID 012002, 2007.

[18] A. Adare, S. Afanasiev, C. Aidala et al., "Direct photon production in $p+p$ collisions at $\sqrt{s} = 200$ GeV at midrapidity," *Physical Review D*, vol. 86, no. 7, Article ID 072008, 2012.

[19] P. Aurenche, A. Douiri, R. Baier, M. Fontannaz, and D. Schiff, "Prompt photon production at large pT in QCD beyond the leading order," *Physics Letters B*, vol. 140, no. 1-2, pp. 87–92, 1984.

[20] P. Aurenche, R. Baier, M. Fontannaz, and D. Schiff, "Prompt photon production at large pT scheme invariant QCD predictions and comparison with experiment," *Nuclear Physics, Section B*, vol. 297, no. 4, pp. 661–696, 1988.

[21] J. F. Owens, "Large-momentum-transfer production of direct photons, jets, and particles," *Reviews of Modern Physics*, vol. 59, no. 2, pp. 465–503, 1987.

[22] P. Aurenche, R. Baier, and M. Fontannaz, "Prompt photon production at colliders," *Physical Review D*, vol. 42, no. 5, pp. 1440–1449, 1990.

[23] H. Baer, J. Ohnemus, and J. F. Owens, "Next-to-leading-logarithm calculation of direct photon production," *Physical Review D*, vol. 42, no. 1, pp. 61–71, 1990.

[24] E. L. Berger and J. Qiu, "Calculations of prompt-photon production in QCD," *Physical Review D*, vol. 44, no. 7, pp. 2002–2024, 1991.

[25] L. E. Gordon and W. Vogelsang, "Polarized and unpolarized isolated prompt photon production beyond the leading order," *Physical Review D*, vol. 50, no. 3, pp. 1901–1916, 1994.

[26] J. Cleymans, E. Quack, K. Redlich, and D. Srivastava, "Prompt photon production in p-p collisions," *International Journal of Modern Physics A*, vol. 10, pp. 2941–2960, 1995.

[27] P. Aurenche, M. Fontannaz, J. P. Guillet, B. Kniehl, E. Pilon, and M. Werlen, "A critical phenomenological study of inclusive photon production in hadronic collisions," *European Physical Journal C*, vol. 9, no. 1, pp. 107–119, 1999.

[28] G. P. Skoro, M. Zupan, and M. V. Tokarev, "Asymmetry of prompt photon production in collisions at RHIC," *Il Nuovo Cimento A*, vol. 112, no. 8, pp. 809–818, 1999.

[29] M. Fontannaz, J. P. Guillet, and G. Heinrich, "Isolated prompt photon photoproduction at NLO," *European Physical Journal C*, vol. 21, no. 2, pp. 303–312, 2001.

[30] S. Catani, M. Fontannaz, J.-P. Guillet, and E. Pilon, "Cross section of isolated prompt photons in hadron-hadron collisions," *Journal of High Energy Physics*, vol. 6, no. 5, pp. 667–700, 2002.

[31] P. Bolzoni, S. Forte, and G. Ridolfi, "Renormalization group approach to Sudakov resummation in prompt photon production," *Nuclear Physics B*, vol. 731, no. 1-2, pp. 85–108, 2005.

[32] P. Aurenche, J. P. Guillet, E. Pilon, M. Werlen, and M. Fontannaz, "Recent critical study of photon production in hadronic collisions," *Physical Review D*, vol. 73, no. 9, Article ID 094007, 2006.

[33] A. V. Lipatov and N. P. Zotov, "Charm photoproduction at DESY HERA: $k_T$ factorization versus experimental data," *Physical Review D*, vol. 75, no. 1, Article ID 014028, 2007.

[34] S. P. Baranov, A. V. Lipatov, and N. P. Zotov, *J. Phys. G*, vol. 36, Article ID 125008, 2009.

[35] M. D. Schwartz, "Precision direct photon spectra at high energy and comparison to the 8 TeV ATLAS data," *JHEP*, vol. 1609, article 005, 2016.

[36] S. Odaka and Y. Kurihara, "Consistent simulation of direct-photon production in hadron collisions including associated two-jet production," *Modern Physics Letters A*, vol. 31, no. 16, Article ID 1650099, 2016.

[37] A. V. Lipatov and M. A. Malyshev, "Reconsideration of the inclusive prompt photon production at the LHC with $k_T$-factorization," *Physical Review D*, vol. 49, no. 3, Article ID 034020, 2016.

[38] T. Ježo, M. Klasen, and F. König, "Prompt photon production and photon-hadron jet correlations with POWHEG," *Journal of High Energy Physics*, vol. 2016, no. 11, article 033, 2016.

[39] A. Kohara and C. Marquet, "Prompt photon production in double-Pomeron-exchange events at the LHC," *Physics Letters B*, vol. 757, pp. 393–398, 2016.

[40] J. M. Campbell, R. K. Ellis, and C. Williams, "Direct photon production at next-to-next-to-leading order," https://arxiv.org/abs/1612.04333.

[41] M. Goharipour and H. Mehraban, "Study of isolated prompt photon production in p-Pb collisions for the ALICE kinematics," *Physical Review D*, vol. 95, no. 5, Article ID 054002, 2017.

[42] F. D. Aaron, A. Aktas, C. Alexa et al., "Measurement of isolated photon production in deep-inelastic scattering at HERA," *The European Physical Journal C*, vol. 54, no. 3, pp. 371–387, 2008.

[43] S. Chekanov, M. Derrick, S. Magill et al., "Measurement of isolated photon production in deep inelastic *ep* scattering," *Physics Letters B*, vol. 687, no. 1, pp. 16–25, 2010.

[44] H. Abramowicz, I. Abt, L. Adamczyk et al., "Photoproduction of isolated photons, inclusively and with a jet, at HERA," *Physics Letters B*, vol. 730, pp. 293–301, 2014.

[45] P. Aurenche, R. Baier, M. Fontannaz, J. F. Owens, and M. Werlen, "Gluon content of the nucleon probed with real and virtual photons," *Physical Review D*, vol. 39, no. 11, pp. 3275–3286, 1989.

[46] W. Vogelsang and A. Vogt, "Constraints on the proton's gluon distribution from prompt photon production," *Nuclear Physics, Section B*, vol. 453, no. 1-2, pp. 334–352, 1995.

[47] R. Ichou and D. d'Enterria, "Sensitivity of isolated photon production at TeV hadron colliders to the gluon distribution in the proton," *Physical Review D*, vol. 82, no. 1, Article ID 014015, 2010.

[48] D. D'Enterria and J. Rojo, "Quantitative constraints on the gluon distribution function in the proton from collider isolated-photon data," *Nuclear Physics B*, vol. 860, no. 3, pp. 311–338, 2012.

[49] A. Aleedaneshvar, M. Goharipour, and S. Rostami, "The impact of intrinsic charm on the parton distribution functions," *The European Physical Journal A*, vol. 52, article 352, 2016.

[50] S. J. Brodsky, A. Kusina, F. Lyonnet, I. Schienbein, H. Spiesberger, and R. Vogt, "A Review of the Intrinsic Heavy Quark Content of the Nucleon," *Advances in High Energy Physics*, vol. 2015, Article ID 231547, 12 pages, 2015.

[51] S. Rostami, M. Goharipour, and A. Aleedaneshvar, "Impact of intrinsic charm models on production of $\gamma$+c-jet differential cross section at LHC and Tevatron," *PoS DIS*, vol. 2016, article 044, 2016.

[52] S. Rostami, M. Goharipour, and A. Aleedaneshvar, "Role of the intrinsic charm content of the nucleon from various light-cone models on $\gamma$+c-jet production," *Chinese Physics C*, vol. 40, no. 12, Article ID 123104, 2016.

[53] G. L. Bayatian, S. Chatrchyan, G. Hmayakyan et al., "CMS physics technical design report, volume II: physics performance," *Journal of Physics G: Nuclear and Particle Physics*, vol. 34, no. 6, p. 995, 2007.

[54] G. Aad, B. Abbott, J. Abdallah et al., "Measurement of Higgs boson production in the diphoton decay channel in *pp* collisions at center-of-mass energies of 7 and 8 TeV with the ATLAS detector," *Physical Review D*, vol. 90, no. 11, Article ID 112015, 2014.

[55] Z. Heng, "A 125 GeV Higgs and its diphoton signal in different SUSY models: a mini review," *Advances in High Energy Physics*, vol. 2012, Article ID 312719, 17 pages, 2012.

[56] J. W. Fan, J.-Q. Tao, Y.-Q. Shen et al., "Study of diphoton decays of the lightest scalar Higgs boson in the Next-to-Minimal Supersymmetric Standard Model," *Chinese Physics C*, vol. 38, no. 7, Article ID 073101, 2014.

[57] A. Adare, S. Afanasiev, C. Aidala et al., "Enhanced production of direct photons in Au+Au collisions at $\sqrt{s_{NN}}$ = 200 GeV and implications for the initial temperature," *Physical Review Letters*, vol. 104, no. 13, Article ID 132301, 2010.

[58] S. Afanasiev, A. Adare, S. Adler et al., "Measurement of Direct Photons in Au+Au Collisions at $\sqrt{s_{NN}}$ = 200 GeV," *Physical Review Letters*, vol. 109, no. 15, Article ID 152302, 2012.

[59] A. Adare, S. S. Adler, S. Afanasiev et al., "Direct photon production in $d$ + Au collisions at $\sqrt{s_{NN}}$ = 200 GeV," *Physical Review C*, vol. 87, no. 5, Article ID 054907, 8 pages, 2013.

[60] B. Müller, "PHENIX and the quest for the quark-gluon plasma," *Progress of Theoretical and Experimental Physics*, no. 3, Article ID 03A103, 2015.

[61] D. Morrison and J. L. Nagle, "PHENIX: beyond 15 years of discovery," *Progress of Theoretical and Experimental Physics*, vol. 2015, no. 3, 2015.

[62] C. Yang, "Direct photon production in Au + Au collisions at $\sqrt{s_{NN}}$ = 200 GeV at STAR," *Nuclear Physics A*, vol. 931, pp. 691–695, 2014.

[63] S. Chatrchyan, V. Khachatryan, A. M. Sirunyan et al., "Measurement of isolated photon production in pp and PbPb collisions at $\sqrt{s_{NN}}$ = 2.76," *Physics Letters B*, vol. 710, no. 2, pp. 256–277, 2012.

[64] M. Wilde, "Measurement of direct photons in pp and Pb–Pb collisions with ALICE," *Nuclear Physics A*, vol. 904-905, pp. 573c–576c, 2013.

[65] J. Adam, D. Adamová, M. M. Aggarwal et al., "Direct photon production in Pb–Pb collisions at $\sqrt{s_{\mathrm{NN}}}$ = 2.76," *Physics Letters B*, vol. 754, pp. 235–248, 2016.

[66] G. Aad, B. Abbott, J. Abdallah et al., "Centrality, rapidity, and transverse momentum dependence of isolated prompt photon production in lead-lead collisions at $\sqrt{s_{NN}}$ = 2.76 TeV measured with the ATLAS detector," *Physical Review C*, vol. 93, no. 3, Article ID 034914, 28 pages, 2016.

[67] N. Novitzky, "Experimental overview of direct photon results in heavy ion collisions," *Nuclear and Particle Physics Proceedings*, vol. 276-278, pp. 66–71, 2016.

[68] W. Dai, S. Y. Chen, B. W. Zhang, and E. K. Wang, "Cold nuclear matter effects on isolated prompt photon and isolated prompt photon+jet productions in relativistic heavy-ion collisions," *Communications in Theoretical Physics*, vol. 59, no. 3, p. 349, 2013.

[69] I. Helenius, K. J. Eskola, and H. Paukkunen, "Centrality dependence of inclusive prompt photon production in d+Au, Au+Au, p+Pb, and Pb+Pb collisions," *Journal of High Energy Physics*, vol. 2013, no. 5, 2013.

[70] E. V. Shuryak, "Quantum chromodynamics and the theory of superdense matter," *Physics Reports*, vol. 61, no. 2, pp. 71–158, 1980.

[71] D. D'Enterria, "Quark-gluon matter," *Journal of Physics G: Nuclear and Particle Physics*, vol. 34, no. 7, article S04, 2007.

[72] J. Jalilian-Marian, K. Orginos, and I. Sarcevic, "Nuclear effects in prompt photon production at the Large Hadron Collider," *Nuclear Physics A*, vol. 700, no. 1-2, pp. 523–538, 2002.

[73] B. Z. Kopeliovich, A. H. Rezaeian, and I. Schmidt, "Azimuthal asymmetry of prompt photons in nuclear collisions," *Nuclear Physics A*, vol. 807, no. 1-2, pp. 61–70, 2008.

[74] Y. Kumar and S. S. Singh, "Free energy evolution and photon radiation from QGP," *ISRN High Energy Physics*, vol. 2013, Article ID 156747, 8 pages, 2013.

[75] M. Mandal and P. Roy, "Some aspects of anisotropic quark-gluon plasma," *Advances in High Energy Physics*, vol. 2013, Article ID 371908, 20 pages, 2013.

[76] S. Somorendro Singh and Y. Kumar, "Direct photon production at finite chemical potential from quark-gluon plasma," *International Journal of Modern Physics A*, vol. 30, no. 3, Article ID 1550020, 2015.

[77] M. Hirai, S. Kumano, and T.-H. Nagai, "Determination of nuclear parton distribution functions and their uncertainties at next-to-leading order," *Physical Review C*, vol. 76, Article ID 065207, 2007.

[78] K. Eskola, H. Paukkunen, and C. Salgado, "EPS09—a new generation of NLO and LO nuclear parton distribution functions," *Journal of High Energy Physics*, vol. 2009, no. 4, article 065, 2009.

[79] D. De Florian, R. Sassot, P. Zurita, and M. Stratmann, "Global analysis of nuclear parton distributions," *Physical Review D*, vol. 85, no. 7, Article ID 074028, 2012.

[80] H. Khanpour and S. Atashbar Tehrani, "Global analysis of nuclear parton distribution functions and their uncertainties at next-to-next-to-leading order," *Physical Review D*, vol. 93, no. 1, Article ID 014026, 2016.

[81] K. Kovarik, A. Kusina, T. Ježo et al., "nCTEQ15: global analysis of nuclear parton distributions with uncertainties in the CTEQ framework," *Physical Review D*, vol. 93, no. 8, Article ID 085037, 2016.

[82] M. Hirai, "Update of HKN nuclear PDFs," in *Proceedings of the 10th International Workshop on Neutrino-Nucleus Interactions in Few-GeV Region (NuInt '15)*, vol. 12, 2016.

[83] F. Arleo and T. Gousset, "Measuring gluon shadowing with prompt photons at RHIC and LHC," *Physics Letters B*, vol. 660, no. 3, pp. 181–187, 2008.

[84] C. B. Mariotto and V. P. Gonçalves, "Nuclear shadowing and prompt photons in hadronic collisions at ultrarelativistic energies," *Physical Review C*, vol. 78, Article ID 037901, 2008.

[85] F. Arleo, K. J. Eskola, H. Paukkunen, and C. A. Salgado, "Inclusive prompt photon production in nuclear collisions at RHIC and LHC," *Journal of High Energy Physics*, vol. 2011, article 55, 2011.

[86] I. Helenius, K. J. Eskola, and H. Paukkunen, "Observation of $Z$ production in proton-lead collisions at LHCb," *JHEP*, vol. 1409, article 030, 2014.

[87] W. Celmaster and D. Sivers, "Factorization prescriptions and phenomenological applications of the parton model," *Annals of Physics*, vol. 143, no. 1, pp. 1–32, 1982.

[88] J. C. Collins, D. E. Soper, and G. F. Sterman, "Factorization of hard processes in QCD," *Advanced Series on Directions in High Energy Physics*, vol. 5, pp. 1–91, 1989.

[89] R. Brock, G. Sterman, J. Smith et al., "Handbook of perturbative QCD," *Reviews of Modern Physics*, vol. 67, no. 1, article 157, 1995.

[90] G. C. Nayak, "Proof of factorization using background field method of QCD," *Annals of Physics*, vol. 325, no. 2, pp. 514–518, 2010.

[91] ATLAS Collaboration, "Study of inclusive isolated-photon production in pp collisions at $\sqrt{s}$ = 13 TeV with the ATLAS detector," ATL-PHYS-PUB-2015-016.

[92] S. Dulat, T.-J. Hou, J. Gao et al., "New parton distribution functions from a global analysis of quantum chromodynamics," *Physical Review D*, vol. 93, no. 3, Article ID 033006, 2016.

[93] L. A. Harland-Lang, A. D. Martin, P. Motylinski, and R. S. Thorne, "Parton distributions in the LHC era: MMHT 2014 PDFs," *European Physical Journal C*, vol. 75, no. 5, article 204, 2015.

[94] R. D. Ball, V. Bertone, S. Carrazza et al., "Parton distributions for the LHC run II," *JHEP*, vol. 1504, article 040, 2015.

[95] H. Abramowicz, L. Abt, K. Adamczy et al., "Combination of measurements of inclusive deep inelastic $e^{\pm}p$ scattering cross sections and QCD analysis of HERA data," *The European Physical Journal C*, vol. 75, no. 12, article 580, 2015.

[96] P. Jimenez-Delgado and E. Reya, "Delineating parton distributions and the strong coupling," *Physical Review D*, vol. 89, no. 7, Article ID 074049, 2014.

[97] S. Frixione, "Isolated photons without fragmentation contribution," in *Proceedings of the 29th International Conference on High-Energy physics*, vol. 1, pp. 790–794, Vancouver, Canada, July 1998.

[98] Z. Belghobsi, M. Fontannaz, J.-P. Guillet, G. Heinrich, E. Pilon, and M. Werlen, "Photon-jet correlations and constraints on fragmentation functions," *Physical Review D*, vol. 79, no. 11, Article ID 114024, 2009.

[99] T. Becher, G. Bell, C. Lorentzen, and S. Marti, "Transverse-momentum spectra of electroweak bosons near threshold at NNLO," *Journal of High Energy Physics*, vol. 2014, no. 2, article 4, 2014.

[100] A. Buckley, J. Ferrando, S. Lloyd et al., "LHAPDF6: parton density access in the LHC precision era," *The European Physical Journal C*, vol. 75, no. 3, article 132, 2015.

[101] L. Bourhis, M. Fontannaz, and J. P. Guillet, "Quark and gluon fragmentation functions into photons," *European Physical Journal C*, vol. 2, no. 3, pp. 529–537, 1998.

[102] R. Blair, B. Brelier, F. Bucci, S. Chekanov, M. Stockton, and M. Tripiana, "NLO theoretical predictions for photon measurements using the PHOX generators," Tech. Rep. CERN-OPEN-2011-041, 2011, http://cds.cern.ch/record/1379880/files/CERN-OPEN-2011-041.pdf.